Signaling pathways and cell mechanics involved in wound closure by epithelial cell sheets

Gabriel Fenteany*†, Paul A. Janmey‡ and Thomas P. Stossel*

Background: Sheets of cells move together as a unit during wound healing and embryonic tissue movements, such as those occurring during gastrulation and neurulation. We have used epithelial wound closure as a model system for such movements and examined the mechanisms of closure and the importance of the Rho family of Ras-related small GTPases in this process.

Results: Wounds induced in Madin–Darby canine kidney (MDCK) epithelial cell monolayers close by Rac- and phosphoinositide-dependent cell crawling, with formation of lamellipodia at the wound margin, and not by contraction of a perimarginal actomyosin purse-string. Although Rho-dependent actin bundles usually form at the margin, neither Rho activity nor formation of these structures is required for wound closure to occur at a normal rate. Cdc42 activity is also not required for closure. Inhibition of Rho or Cdc42 results, however, in statistically significant decreases in the regularity of wound closure, as determined by the ratio of wound margin perimeter over the remaining denuded area at different times. The Rac-dependent force generation for closure is distributed over several rows of cells from the wound margin, as inhibition of motility in the first row of cells alone does not inhibit closure and can be compensated for by generation of motile force in cells behind the margin. Furthermore, we observed high levels of Rac-dependent actin assembly in the first few rows of cells from the wound margin.

Conclusions: Wounds in MDCK cell sheets do not close by purse-string contraction but by a crawling behavior involving Rac, phosphoinositides and active movement of multiple rows of cells. This finding suggests a new distributed mode of signaling and movement that, nevertheless, resembles individual cell motility. Although Rho and Cdc42 activities are not required for closure, they have a role in determining the regularity of closure.

Addresses: *Division of Hematology, Brigham and Women's Hospital, Department of Medicine, Harvard Medical School, 221 Longwood Avenue, Boston, Massachusetts 02115, USA. ‡Department of Physiology and Institute for Medicine and Engineering, Vagelos Research Laboratories, University of Pennsylvania, Philadelphia, Pennsylvania 19104, USA.

†Present address: Department of Chemistry, University of Illinois, Chicago, Illinois 60607, USA.

Correspondence: Gabriel Fenteany
E-mail: fenteany@slsiris.harvard.edu

Received: **3 April 2000**
Accepted: **30 May 2000**

Published: **21 June 2000**

Current Biology 2000, 10:831–838

0960-9822/00/$ – see front matter

Background

The crawling movements of cells depend on actin filament reorganization, assembly and disassembly (reviewed in [1,2]). Individual members of the Rho family of small GTPases induce modular versions of these changes in actin state, leading to particular cell-surface mechanics. The introduction of reagents for probing GTPase function *in vivo* now enables us to try to decipher how actin remodeling powers cell movement.

The Rho-family proteins Rho, Rac and Cdc42 have a range of normal cellular roles, of which, those relating to the regulation of the actin cytoskeleton in cell shape changes and motility are best characterized (reviewed in [3,4]). In fibroblasts, Rho proteins are associated generally with formation of contractile actomyosin bundles and stress fibers and the assembly of focal adhesion complexes [5]. Rac proteins are associated with formation of lamellipodia and membrane ruffling [6], as well as the modulation of cadherin-based cell–cell adhesion [7]. Cdc42 is associated with formation of filopodia [8] and control of cell polarity [9].

The role of these small GTPases in the movement of epithelial cell sheets, which are essential for normal embryonic development and the healing of tissue wounds, has been less well characterized than their roles in individual cell movement. The movement of embryonic cell sheets is very similar to wound closure in animals, tissue explants and cell culture models in respect of the signaling molecules involved, the changes in cell morphology and mechanisms of motility (reviewed in [10,11]).

Investigators have proposed two distinct mechanisms to account for wound closure in epithelial cell sheets. In the first, demonstrated in the wounded embryonic chick wing bud, a circumferential ring of actin bundles mediates a contractile response that draws the wound edges together, as a purse-string closes a purse [12]. This process requires the function of Rho but not of Rac [13]. In the second,

which is characteristic of epithelial cell sheets in adult organisms, active protrusion of filopodia and ruffling lamellae occurs at the edge of the wound, resembling the crawling behavior of free cells rather than a purse-string contractile event (reviewed in [14]).

In other cases, the movement of a cell sheet exhibits aspects of both purse-string contraction and protrusion-based crawling, either simultaneously or at different stages. Closure of small wounds in cultures of intestinal epithelial cells involves formation of both lamellipodia and purse-string structures [15] and is dependent on the function of Rho [16]. Although not an example of wound closure, ventral enclosure in the nematode *Caenorhabditis elegans* is descriptively very similar and occurs in two stages, one accompanied by filopodial extension, the other by an apparent purse-string contraction [17]. Similarly, dorsal closure in the fruit fly *Drosophila melanogaster* appears to involve a purse-string mechanism [18,19], although it is also dependent on the function of Rac [20].

When wounds close by a purse-string mechanism, the obvious driving force is the contraction of actomyosin complexes. For wound closure by crawling, the mechanics are less clear. Do the cells at the wound edge pull the sheet in centripetally, do cells behind the margin (submarginal cells) push, or do both processes occur? As even in these kinds of wounds, there are often dense actin bundles at the wound margins, does some component of purse-string activity contribute to the forces required? To address these questions, we have investigated the relative importance of different Rho-family GTPases during wound closure in cell sheets of the MDCK epithelial cell line. We find that the dominant mechanism of closure is crawling rather than purse-string contraction. By selectively inhibiting crawling in the first row of cells at the margin, we show that crawling behavior mediated by actin assembly in cells behind the margin contributes importantly to the force for wound closure. We also provide evidence that raised levels of actin assembly occur several cell rows in from the wound margin.

Results

Cells at the wound margin extend Rac- and phosphoinositide-dependent lamellipodia

Wounding induces migration of the remaining intact MDCK cell sheet into the gap. As previously observed, cell proliferation does not contribute to the filling of small wounds in this system [21]. After the wound is covered and the cells cease to migrate, however, cell division in the former wound area occurs (data not shown). The images of wounds shown in Figures 1–6 are representative of wounds of different sizes and shapes, and results are summarized in Table 1.

Cells at the wound margin in MDCK cell monolayers extend lamellipodia in the direction of movement into the denuded area, followed by tandem movement of the submarginal cells (Figures 1,4,5a). During this process, the cell sheet maintains its coherence, yet displacement of cells relative to one another occurs in both wounded and unwounded monolayers over a time scale of hours. Microinjection of dominant-negative Rac1 protein (N17Rac1) into all the cells in the first three rows at the wound margin completely abolishes wound closure (Figures 2,5b), whereas

Figure 1

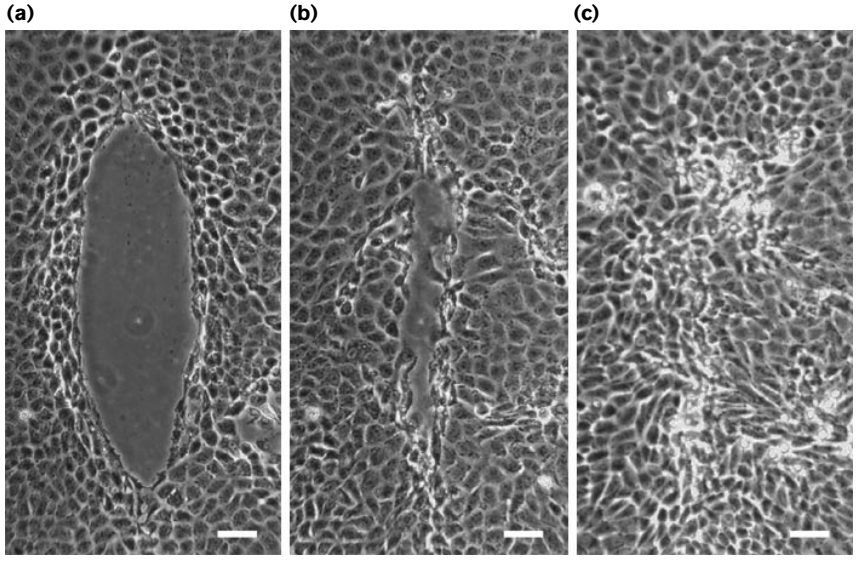

Wound closure in Madin–Darby canine kidney (MDCK) epithelial cell monolayers. **(a–c)** Phase-contrast micrographs of MDCK cells after wounding and microinjection with 2.5 mg/ml solution of OG dextran into the first three rows of cells around the wound margin (concentration in cells after microinjection is ~1/10th that of the microinjected solution or ~250 μg/ml). Cells are shown (a) immediately after wounding and microinjection, (b) after 6 h, and (c) after 18 h. The scale bar represents 50 μm. All figures for each treatment in this paper are representative of experiments performed in triplicate on at least three separate occasions ($n \geq 9$).

Figure 2

Inhibition of Rac in the first three rows of cells behind the margin abolishes wound closure. **(a–c)** Phase-contrast micrographs of MDCK cells after wounding and microinjection with 50 μM solution of dominant-negative Rac (N17Rac1; co-injected with OG dextran) into the first three rows of cells around the wound margin. Cells are shown (a) immediately after wounding and microinjection, (b) after 6 h, (c) after 18 h. The scale bar represents 50 μm.

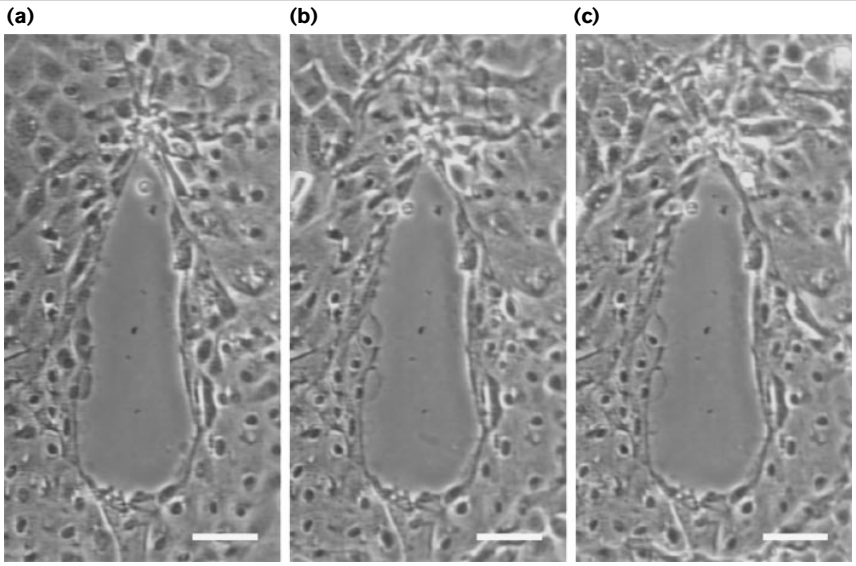

microinjection of N17Rac1 into the first row of cells only does not (Figures 3,5c). Microinjection of dextran conjugated to the fluorescent dye Oregon Green (OG dextran), to make microinjected cells visible, has no effect on formation of lamellipodia or perimarginal actin bundles (Figures 4,5a). Microinjection of a gelsolin-derived peptide that binds and titrates polyphosphoinositides (PPIs) [22] into the first three rows of cells also completely inhibits wound closure (Figure 5d). In contrast, lamellipodium formation and wound closure are not inhibited by microinjection of C3 exoenzyme (an inactivator of RhoA, RhoB and RhoC; Figure 5e) or dominant-negative Cdc42 (N17Cdc42; Figure 5f).

Cells behind the wound margin can drive wound closure

Microinjection of N17Rac1 solely into the cells in the first cell row at the wound margin does not prevent wound closure; this treatment does, however, inhibit formation of lamellipodia in the first row (Figures 3,5c). These results are independent of wound size and shape. The cells of the

Figure 3

Inhibition of Rac in the first row of cells only does not prevent wound closure. **(a–c)** Phase-contrast micrographs of MDCK cells immediately after wounding and microinjection with 50 μM solution of dominant-negative Rac (N17Rac1; co-injected with OG dextran) into the first row of cells only around the wound margin. Cells are shown (a) immediately after wounding and microinjection, (b) after 6 h, and (c) after 18 h. The scale bar represents 50 μm.

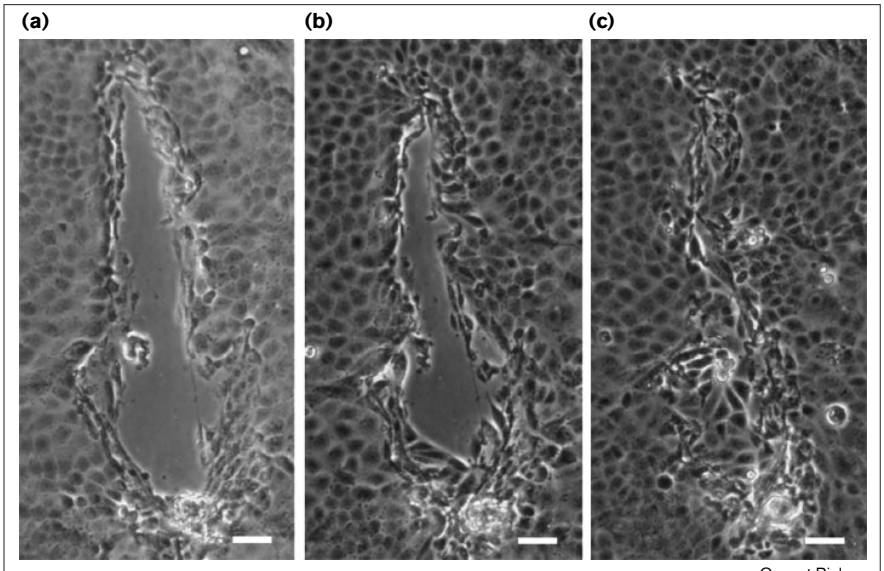

Figure 4

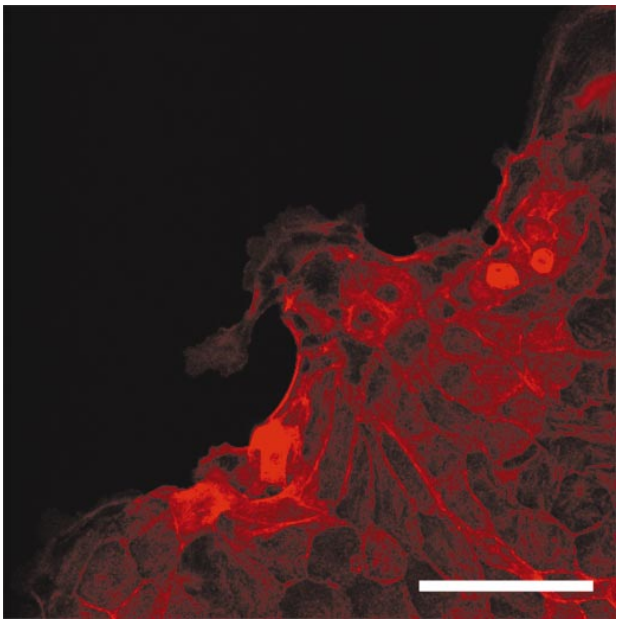

Protrusive activity and actin organization at the wound margin. A confocal micrograph of MDCK cells fixed, treated with the detergent Triton X-100 to extract soluble material, and stained with rhodamine-conjugated phalloidin 1 h after wounding and microinjection with 2.5 mg/ml OG dextran into the first three rows of cells. Scale bar represents 50 μm.

first row narrow along their axis perpendicular to the wound margin as they move inward without forming observable protrusions. At later stages, some of the cells behind the margin move between the first-row cells and enter the remaining bare area. Attempts at visualizing protrusive structures in submarginal cells at various depths in the *z*-axis, using confocal microscopy, do not reveal any evidence of lamellipodium-like structures in the cells behind the first row. The presence of very small or transient structures eluding detection by confocal microscopy cannot be ruled out, however. Mechanically killing the first few rows of cells by puncturing them with a wide-tip glass needle also does not inhibit wound closure. The damaged cells remain intact but do not prevent undamaged submarginal cells from pushing in and closing the wound.

Actin filament assembly is detectable in cells several rows from the wound margin

Figure 6a shows that 6 hours after wounding and microinjection of OG dextran into the first three cell rows behind the wound margin, detergent-resistant rhodamine-conjugated actin is accumulated at high concentration in several rows of permeabilized cells behind the margin. The fluorescence intensity then tapers off with increasing distance from the margin. Unwounded controls display a low background level of actin incorporation similar to that observed at a greater distance from the wound margin. Microinjection of N17Rac1 into the first three rows from the wound margin inhibits actin incorporation (Figure 6b). Cytochalasin B abolishes the staining near the wound margin, indicating that the actin incorporation represents polymerization on new actin nuclei or on pre-existing ends in the fast-growing (barbed) end direction (data not shown). Fixableluorescent dextran does not produce this pattern of

Figure 5

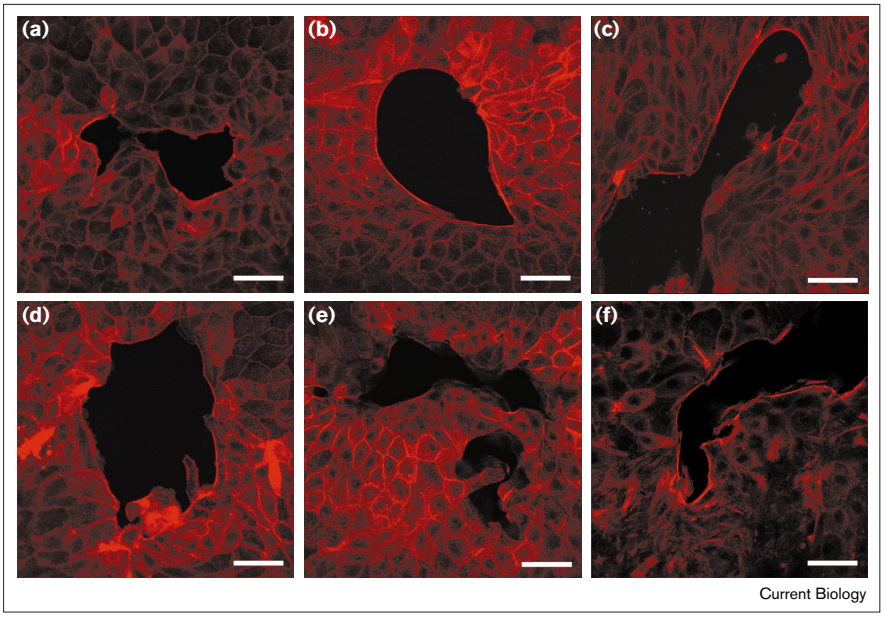

Wound closure, protrusive activity and actin organization at the margin after treatments with various inhibitors of signaling to the actin cytoskeleton. **(a–f)** Confocal micrographs of MDCK cells fixed, treated with Triton X-100 and stained with rhodamine-conjugated phalloidin 6 h after wounding and microinjection with the following compounds into the first three rows of cells, unless otherwise noted: (a) 2.5 mg/ml OG dextran; (b) 50 μM N17Rac1; (c) 50 μM N17Rac1 in the first row of cells only; (d) 50 μM PPI-binding peptide; (e) 5 μM C3 toxin (Rho inhibitor); (f) 50 μM N17Cdc42. The scale bar represents 50 μm.

Figure 6

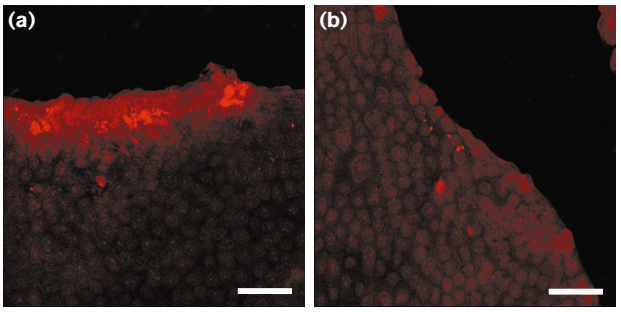

Rac-dependent actin assembly in multiple rows of cells from the wound margin. **(a,b)** Confocal micrographs of MDCK cells showing rhodamine-conjugated actin incorporation into the insoluble cytoskeleton (incorporation started 6 h after wounding). (a) Incorporation of rhodamine–actin into filaments 6 h after wounding and microinjection of OG dextran alone into the first three rows of cells from the wound margin. (b) Incorporation of rhodamine–actin into filaments 6 h after wounding and microinjection of N17Rac1 into the first three rows of cells from the wound margin. Parallel treatment with lysine-fixable OG dextran did not produce this pattern of differential staining, and cytochalasin B (an inhibitor of actin polymerization from the barbed end of filaments or nuclei) inhibited the rhodamine–actin staining (data not shown). The scale bar represents 50 μm.

Table 1

Regularity of wound closure for each treatment.

Treatment	Percentage change in (wound perimeter length/remaining bare area)
Control	30.2 ± 8.1
N17Rac1 (three rows)	9.7 ± 9.1*
N17Rac1 (first row)	21.4 ± 12.6
PPI-binding peptide (three rows)	3.4 ± 7.9*
C3 toxin (three rows)	49.4 ± 15.1*
N17Cdc42 (three rows)	51.5 ± 8.8*

The regularity of wound closure was measured as a percentage change in the ratio of wound perimeter length over the remaining bare area from 0 to 6 h. Numbers are given as mean ± SD with $n = 9$ in each case. Asterisks indicate statistically significant differences ($p < 0.05$) from control values as determined by Student's t test.

differential staining (data not shown), further indicating that the increased actin incorporation at the wound margin is not a result of greater permeability at this site.

Formation of actin bundles at the wound margin depends on Rho activity but is not necessary for wound closure

Although microinjection with either dominant-negative Rac1 (Figure 5b) or the PPI-binding peptide (Figure 5d) completely abolishes formation of lamellipodia, this procedure has little or no effect on accumulation of actin bundles at the wound margin, as shown by staining with rhodamine-conjugated phalloidin. Conversely, microinjection with C3 exoenzyme does not inhibit lamellipodial extension and wound closure, but does reduce formation of perimarginal actin bundles (Figure 5e). Particularly intense staining of actin bundles is observed in cells immediately adjacent to those that are extending protrusions (Figure 4). Confocal imaging along the z-axis also reveals staining of actin bundles apical to and just behind the lamellipodium in protrusive cells, but this staining is much weaker than that found in the adjacent cells lacking protrusions. Microinjection of N17Cdc42 has no effect on formation of either lamellipodia or perimarginal actin bundles (Figure 5f).

Rho and Cdc42 activities are important for regular wound closure

Although rates of closure for wounds of similar size and shape within each treatment are variable (except for the treatments where closure is completely abrogated), inhibition of Rho or Cdc42 activities results in statistically significant differences in the regularity of wound closure, as measured by the change in the ratio of wound perimeter to the remaining bare area in the 6 hours after wounding (Table 1).

Discussion

Wound closure in the MDCK epithelial cell system shares many mechanistic features with the crawling behavior of free cells, and we have found this to be true of wounds of different sizes and shapes for each treatment. Cells of the first row around the wound margin extend lamellipodia (Figures 4,5a). Not all cells in the first row display this protrusive activity at the same time; rather, lamellipodial activity is dynamic and variable. A given cell may protrude and appear to pull neighboring cells along at one point in time, while later, another cell may appear more active and motile, again pulling its neighbors along. The smooth and regular contour of the leading edge of cells adjacent to the most actively protrusive cells at the wound margin implies a tension-based continuity of force from an active cell to its neighbors. Furthermore, the pattern of actin staining shows that perimarginal actin bundles (also sometimes referred to as actin cables in the literature) appear thicker in cells adjacent to a cell extending a lamellipodium. This suggests the possibility of an active bundle-based pulling of adjacent cells in the first row by the active cells.

Inhibition of Rac activity in the first three rows completely abolishes both lamellipodium formation and wound closure (Figures 2,5b). Furthermore, inhibition of PPI signaling using a PPI-binding and titrating peptide has an effect identical to that of inhibition of Rac activity with dominant-negative Rac1. Phosphoinositides are important mediators of actin assembly, whether it occurs by *de novo* nucleation of actin filament assembly by the Arp2/3 complex, promoted by activated Cdc42 [23,24], or

by uncapping of pre-existing actin filaments downstream of Rac signaling [25]. In our system, Cdc42 inhibition does not block wound closure, implying a more important role for Rac pathways.

MDCK cell monolayers, like epithelial sheets in intact organisms, maintain strong cell–cell adhesion even during wound closure, and so the mechanics of closure in these monolayers displays properties different from those of cells that migrate predominantly as individual cells or only weakly adhering to other cells. A fundamental question regarding the movement of the cell sheet in wound healing is whether only cells at the wound margin generate active force — in effect, pulling passive submarginal cells with them as they move forward — or whether the generation of active force is more distributed between rows, both at the wound margin and behind it. Inhibition of lamellipodial extension and observable crawling morphology in the first row of cells alone by Rac inhibition does not appear to affect the rate of closure of wounds of different sizes and shapes. Persistent migration occurs despite the reduction in observable lamellipodial extension in the first-row cells. These results imply that cells behind the margin can generate force independently of the first row.

Confocal microscopy does not reveal the presence of lamellipodia in the active cells behind the first row. It is possible that these submarginal cells extend cryptic lamellipodia that are too small or transient to observe or that are wedged under the cells just in front of them. This idea would be consistent with the fact that adherens junctions tend to be apical in epithelia, and thus the more basal extension of tiny lamellipodia could be hidden under the apical actin-linked contacts. On the other hand, these submarginal cells may push directly against the more forward cells without clear formation of protrusive structures.

Formation of protrusive structures like lamellipodia and filopodia during cell crawling requires actin filament assembly (reviewed in [1,2]). Despite our inability to detect obvious surface structures customarily associated with protrusive activity, we have provided evidence that cells up to several rows behind the margin have sites that promote Rac-dependent actin filament assembly, consistent with active actin-based force generation in these cells. The actin filament assembly detected in the fast-growing (barbed) end direction could result from polymerization either from pre-existing ends that are not capped or from new actin nuclei.

Inhibition of Rho activity in wounded MDCK cell monolayers reduces formation of perimarginal actin bundles but not wound closure. These results are inconsistent with a perimarginal purse-string mechanism in this instance. On the other hand, the actin bundles may still have a role in wound closure in that they may help to distribute forces generated by the actively crawling cells to less active neighboring cells, and thus coordinate a smoother inward advance of the whole wound margin. This possibility is supported by our observation that inhibition of Rho activity results in significantly less regular closure of wounds in MDCK cell monolayers (Table 1). Such a contribution of Rho to wound closure could be particularly important in situations in which wounds are larger and affect more than one layer of cells, as in an intact tissue. Our results are in basic agreement with recent work on wound closure in *Xenopus laevis* embryonic animal caps; in the *Xenopus* system, actin bundles form at the wound margin but do not appear to generate the force for closure, whereas cell crawling seems to be critical (L. Davidson and R. Keller, personal communication).

During wound closure in MDCK cell monolayers, protrusions that can be clearly characterized as extended filopodia are not detected. Furthermore, the activity of Cdc42 is dispensable for wound closure in this system. Cdc42 activity does, however, have a role in determining the regularity of closure of wounds in the monolayer (Table 1). Cdc42 activity correlates with formation of filopodia in fibroblasts [8] and is also involved in control of cell polarity, much of this evidence coming from studies in yeast [9].

Scrape wounds induced in rat embryonic fibroblast monolayers close by a Rac-dependent mechanism involving lamellipodial extension [26]. Cdc42 activity enhances closure rates in this study, apparently as a result of a role for Cdc42 in maintaining cell polarity, in possibly localizing lamellipodial activity at the leading edge and in reorienting the Golgi apparatus in the direction of movement. Furthermore, significant inhibition of Rho activity by C3 exoenzyme inhibits the wound closure, apparently by decreasing substrate adhesion and inducing cell retraction; interestingly, increased Rho activity also inhibited wound closure [26]. There are important differences between fibroblast and epithelial wound closure. Fibroblasts tend not to form stable cell sheets and do not consistently migrate as a continuous sheet. In contrast, MDCK cells in wounded monolayers migrate only as a coherent cell sheet. There are a number of distinct types of cell–cell adhesion that maintain contacts between cells in epithelia, such as intermediate filament-linked desmosomes (reviewed in [27]) and adherens junctions that link the actin cytoskeleton to cadherin-based adhesion complexes (reviewed in [28,29]). Epithelia also differ from fibroblast monolayers in possessing tight junctions and having greater direct intercellular communication through gap junctions. Coordination of the activities of Rho-family small GTPases appears important for optimal wound closure in both systems; however, the activities of individual proteins affect wound closure differently in the two cell types.

Our results suggest the possibility that cells can sense their location in a cell sheet and respond accordingly

without being directly adjacent to the sheet edge. Submarginal cells may be able to generate force and initiate migration by sensing a lowered resistance to movement in one direction, or by some chemical or electrical signaling mechanism. In both wounded and unwounded MDCK cell monolayers, time-lapse video microscopy reveals a significant displacement of cells relative to one another on a time scale of hours. This suggests that, even in the absence of any free edges, cells are constantly moving relative to one another. Adhesions may be dynamic, allowing for random 'jostling' as cells push against one another and sample their mechanical environment. When a cell encounters a differential barrier of resistance, it may polarize and move preferentially in the direction of least resistance. Thus, if the row of cells at the edge, between the submarginal cells and the margin, constitutes a lower resistance barrier to movement than the rest of the sheet, the submarginal cells may also move actively in that direction. Another possibility is that wounding or the presence of a free edge itself generates signals that submarginal cells also receive. These two ideas are not mutually exclusive, and cells in a sheet may be coupled both mechanically and chemically in terms of motility.

Conclusions

Wounds in MDCK cell sheets close by Rac- and PPI-dependent cell crawling rather than by purse-string contraction. Rho and Cdc42 activities are not required for wound closure in this system, nor is the formation of perimarginal actin bundles; these activities do, however, have roles in determining the regularity of closure. Several rows of cells behind the wound margin participate in Rac-dependent actin assembly and active force generation. The distributed nature of force generation for closure in this system, identified here for the first time, implies that chemical or mechanical stimuli from the wound edge are transmitted a distance of at least several cell widths from the edge.

Materials and methods

Cells

Madin–Darby canine kidney (MDCK) cells (American Type Culture Collection), were plated onto glass coverslips and grown to confluence in Eagle's Minimum Essential Medium (MEM) with Earle's salts and L-glutamine with 10% fetal bovine serum (FBS). Cells were used for experiments within 2 days of reaching confluence. The coverslips were then placed into a temperature-controlled experimental chamber and maintained at 37°C in the same growth medium by a temperature controller (Medical Systems). Each experiment in this study was performed in triplicate on at least three separate occasions ($n \geq 9$), with parallel control and experimental treatments.

Wounding and microinjection

We made small wounds by scraping the monolayer with a flame-blunted glass microinjection needle attached to a micropositioner and moving the sample stage. We prepared needles for microinjection from borosilicate glass capillaries (TW100F-4; World Precision Instruments) using a needle puller (Narishige) set to generate a 0.5 μm tip diameter on average. Immediately following wounding, we microinjected cells in the appropriate rows from the wound margin with the desired solution. N17Rac1 was kindly provided by Toshifumi Azuma. *Clostridium botulinum* C3 exoenzyme (C3 toxin) was from Calbiochem and N17Cdc42 from Cytoskeleton. The PPI-binding peptide used corresponds to residues 150–169 of human cytoplasmic gelsolin and has been previously characterized [22]. We used a micropositioner and pneumatic injector (Narishige) for microinjection, with injection pressure regulated to introduce volumes not exceeding ~10% of the average cell volume. Oregon Green 488 (OG) dextran (70 kDa) (Molecular Probes) was present in all solutions, making microinjected cells visible by fluorescence.

Time-lapse imaging

We performed time-lapse imaging of cells using a Nikon Diaphot 300 inverted microscope attached to either one of two CCD cameras from Roper Scientific or Sanyo. Images were captured to either a Silicon Graphics O2 workstation running imaging software from Inovision or an Apple Power Macintosh computer connected to a Scion AG-5 frame grabber card and running the NIH Image program. We evaluated cell viability at the end of the experiments by exclusion of Trypan blue (Gibco-BRL).

Rhodamine-conjugated phalloidin staining

To examine the structure of the actin cytoskeleton following each treatment, we wounded confluent MDCK cell monolayers, and the first three rows of cells were microinjected as before with each inhibitor. We fixed cells 6 h after wounding with 3.7% formaldehyde in PBS, permeabilized them in 0.1% Triton X-100 in PBS, stained with 50 nM rhodamine–phalloidin (Molecular Probes) in PBS and mounted them on glass slides. Between each step, we washed the cells three times in PBS. We imaged the slides using a laser scanning confocal microscope from BioRad, taking consecutive slices along the *z*-axis to establish the apico-basal orientation of observed structures.

Actin incorporation by permeabilized cells

For actin incorporation experiments, we used methods similar to those published previously [30]. Six hours after wounding, we incubated the MDCK cells at 37°C for 30 min in a solution containing 0.35 μM actin (1:45 ratio of unlabeled actin to rhodamine–actin (Cytoskeleton)) with 1 mM Tris pH 7.4, 1 mM KCl, 0.2 mM $MgCl_2$, 0.1 mM EGTA (to chelate Ca^{2+} and prevent Ca^{2+}-dependent actin severing), 0.5 mM dithiothreitol, 0.5 mM ATP, 1% NP-40 (for membrane permeabilization) and a protease inhibitor cocktail (Sigma-Aldrich) that included AEBSF, pepstatin A, E-64, bestatin, leupeptin and aprotinin. Cells were then fixed in 3.7% formaldehyde in PBS and soluble material extracted with 0.1% Triton X-100 in PBS, then mounted on glass slides, washing three times in PBS between steps. Fixable lysine-coupled OG dextran (70 kDa) (Molecular Probes) and cytochalasin B (Sigma-Aldrich) were used in separate control experiments. Slides were examined by laser scanning confocal microscopy.

Acknowledgements

We thank Lance Davidson and Ray Keller of the University of Virginia for stimulating discussions and for sharing with us data prior to publication. We acknowledge support from NIH grant HL19429 (T.P.S.) and AR38910 (P.A.J.) and NIH training grant HL07680. G.F. is a SmithKline Beecham Fellow of the Life Sciences Research Foundation.

References

1. Lauffenberger DA, Horwitz AF: **Cell migration: a physically integrated molecular process.** *Cell* 1996, **84:**359-369.
2. Welch MD, Mallavarapu A, Rosenblatt J, Mitchison TJ: **Actin dynamics *in vivo.*** *Curr Opin Cell Biol* 1997, **9:**54-61.
3. Tapon N, Hall A: **Rho, Rac and Cdc42 GTPases regulate the organization of the actin cytoskeleton.** *Curr Opin Cell Biol* 1997, **9:**86-92.
4. Hall A: **Rho GTPases and the actin cytoskeleton.** *Science* 1998, **279:**509-514.
5. Ridley AJ, Hall A: **The small GTP-binding protein rho regulates the assembly of focal adhesions and actin stress fibers in response to growth factors.** *Cell* 1992, **70:**389-399.

6. Ridley A, Paterson H, Johnston C, Diekmann D, Hall A: **The small GTP-binding protein rac regulates growth factor-induced membrane ruffling.** *Cell* 1992, **70:**401-410.
7. Braga VM, Machesky LM, Hall A, Hotchin NA: **The small GTPases Rho and Rac are required for the establishment of cadherin-dependent cell-cell contacts.** *J Cell Biol* 1997, **137:**1421-1431.
8. Kozma R, Ahmed S, Best A, Lim L: **The Ras-related protein Cdc42Hs and bradykinin promote formation of peripheral actin microspikes and filopodia in Swiss 3T3 fibroblasts.** *Mol Cell Biol* 1995, **15:**1942-1952.
9. Johnson DI, Pringle JR: **Molecular characterization of CDC42, a *Saccharomyces cerevisiae* gene involved in the development of cell polarity.** *J Cell Biol* 1990, **111:**143-152.
10. Trinkaus J: *Cells into Organs. The Forces That Shape the Embryo.* Englewood Cliffs, NJ: Prentice Hall; 1984.
11. Nodder S, Martin P: **Wound healing in embryos: a review.** *Anat Embryol* 1997, **195:**215-228.
12. Martin P, Lewis J: **Actin cables and epidermal movement in embryonic wound healing.** *Nature* 1992, **360:**179-183.
13. Brock J, Midwinter K, Lewis J, Martin P: **Healing of incisional wounds in the embryonic chick wing bud: characterization of the actin purse-string and demonstration of a requirement for Rho activation.** *J Cell Biol* 1996, **135:**1097-1107.
14. Martin P: **Wound healing — aiming for perfect skin regeneration.** *Science* 1997, **276:**75-81.
15. Bement W, Forscher P, Mooseker M: **A novel cytoskeletal structure involved in purse string wound closure and cell polarity maintenance.** *J Cell Biol* 1993, **121:**565-578.
16. Santos F, McCormack SA, Guo Z, Oklicany J, Zheng Y, Johnson LR, *et al.*: **Rho proteins play a critical role in cell migration during the early phase of mucosal restitution.** *J Clin Invest* 1997, **100:**216-225.
17. Williams-Masson EM, Malik AN, Hardin J: **An actin-mediated two-step mechanism is required for ventral enclosure in *C. elegans* hypodermis.** *Development* 1997, **124:**2889-2901.
18. Young PE, Richman AM, Ketchum AS, Kiehart DP: **Morphogenesis in *Drosophila* requires nonmuscle myosin heavy chain function.** *Genes Dev* 1993, **7:**29-41.
19. Edwards KA, Demsky M, Montague RA, Weymouth N, Kiehart DP: **GFP-moesin illuminates actin cytoskeleton dynamics in living tissue and demonstrates cell shape changes during morphogenesis in *Drosophila.*** *Dev Biol* 1997, **191:**103-117.
20. Harden N, Loh HY, Chia W, Lim L: **A dominant inhibitory version of the small GTP-binding protein Rac disrupts cytoskeletal structures and inhibits developmental cell shape changes in *Drosophila.*** *Development* 1995, **121:**903-914.
21. Sponsel HT, Breckon R, Hammond W, Anderson RJ: **Mechanisms of recovery from mechanical injury of renal tubular epithelial cells.** *Am J Physiol* 1994, **267:**F257-F264.
22. Janmey PA, Lamb J, Allen PG, Matsudaira PT: **Phosphoinositide-binding peptides derived from the sequences of gelsolin and villin.** *J Biol Chem* 1992, **267:**11818-11823.
23. Ma L, Cantley LC, Janmey PA, Kirschner MW: **Corequirement of specific phosphoinositides and small GTP-binding protein Cdc42 in inducing actin assembly in Xenopus egg extracts.** *J Cell Biol* 1998, **140:**1125-1136.
24. Rohatgi R, Ma L, Miki H, Lopez M, Kirchhausen T, Takenawa T, *et al.*: **The interaction between N-WASP and the Arp2/3 complex links Cdc42-dependent signals to actin assembly.** *Cell* 1999, **16:**221-231.
25. Hartwig J, Bokoch G, Carpenter C, Janmey P, Taylor L, Toker A, *et al.*: **Thrombin receptor ligation and activated Rac uncap actin filament barbed ends through phosphoinositide synthesis in permeabilized platelets.** *Cell* 1995, **82:**643-653.
26. Nobes CD, Hall A: **Rho GTPases control polarity, protrusion, and adhesion during cell movement.** *J Cell Biol* 1999, **144:**1235-1244.
27. Green KJ, Jones JC: **Desmosomes and hemidesmosomes: structure and function of molecular components.** *FASEB J* 1996, **10:**509-514.
28. Vleminckx K, Kemler R: **Cadherins and tissue formation: integrating adhesion and signaling.** *BioEssays* 1999, **21:**211-220.
29. Gumbiner BM: **Regulation of cadherin adhesive activity.** *J Cell Biol* 2000, **148:**399-404.
30. Wiener OD, Servant G, Welch MD, Mitchison TJ, Sedat JW, Bourne HR: **Spatial control of actin polymerization during neutrophil chemotaxis.** *Nature Cell Biol* 1999, **1:**75-81.

Because *Current Biology* operates a 'Continuous Publication System' for Research Papers, this paper has been published on the internet before being printed. The paper can be accessed from http://biomednet.com/cbiology/cub – for further information, see the explanation on the contents page.